Full Paper

Propellants, Explosives, Pyrotechnics

DOI: 10.1002/prep.201300011

Investigation of Blast Performance and Solid Residues for Layered Thermobaric Charges

Waldemar A. Trzciński,*[a] Katarzyna Barcz,[a] Józef Paszula,[a] and Stanisław Cudziło[a]

Abstract: The confined explosion of an annular layered charge composed of a phlegmatized RDX (RDXph) core and an external layer consisting of aluminum powder (Al) or a mixture of ammonium perchlorate (AP) and Al was studied. Experiments were carried out in fully and partially closed structures, i.e., in the explosion chamber of 150 dm^3 in volume and in the 40 m^3 volume bunker with four small holes and a doorway. Two types of aluminum powder were used in the mixtures. Signals of overpressure from two piezoelectric gauges located at the chamber wall were recorded and the influence of aluminum contents and particle size on a quasi-static pressure (QSP) was studied. Moreover, the solid residues from the chamber were analyzed by using SEM, TG/DTA and XRD techniques to determine their structure and composition. Pressure and light histories recorded in the bunker enable us to determine the blast wave characteristics and time-duration of light output. The effect of the charge mass and aluminum particle size on blast wave parameters were investigated. For comparison, the test for RDXph and TNT charges were also carried out.

Keywords: Thermobaric explosives · Layered charges · Confined explosions

1 Introduction

Layered charges consist of cylindrically loaded layers of energetic materials. Usually a core charge is a classic high explosive and outer layers consist of a mixture of fuel and oxidizer or the fuel itself [1–3]. Such materials are classified as enhanced blast explosives (EBX) or thermobaric explosives (TBX). The fuel burning in the products of detonation or oxygen from the air raises the temperature of the cloud of gaseous products and strengthens the blast wave. Differences between the effects of the explosion of TBX and EBX are usually small and therefore often these names are used interchangeably. However, since EBX is primarily to strengthen blast wave, while TBX is to increase in temperature and pressure of the explosion, the classification of charges to a specific type depends on how the fuel is burned after the ending of the detonation. In materials like EBX there is talk about anaerobic combustion reactions, or combustion without oxygen from the air. This means that after passing of the detonation wave, most of the fuel burns in the products of detonation. In materials like TBX, reactions of the fuel and oxygen from the air dominate. This process is described as aerobic burning [4, 5].

Layered explosive charges were described in U.S. patents [1, 2], in which metalized compositions comprising a reactive metal, oxidizer and binder, and optionally a plasticizer and a catalyst were also the patent subject. So-called SFAE charges (*Solid Fuel – Air Explosive*) were patented, i.e., the solid fuel-containing charges of the annual design, and their new explosion properties were claimed. Such charges offer increased thermal effect of the explosion and are able to produce a relatively high pressure (200–400 kPa) lasting longer than 50 ms in environments enabling rapid decline in temperature (free explosion). They are also able to maintain high pressure for a long time in a confined volume with limited amount of oxygen. This type of explosives is characterized by increased reactivity and thermal output and lower ignition temperature [2].

Explosive compositions are claimed in a patent [3], which, as stated by the authors, exposed to a weak shock wave fragment and burn instead of detonate, but the detonation process occurs if they are loaded by a strong shock wave. Also munitions built from these materials became the object of the patent claim, in particular, just thermobaric charges.

Investigation of blast parameters of mixtures of explosive oxidizer and fuel were conducted in Ref. [6], where the characteristics of blast waves generated by the charges containing mixture of ammonium nitrate (AN) and powdered aluminum (Al) were measured. Flaked aluminum or aluminum powder were used in charges with contents 10 and 40 % by weight. It was demonstrated that the blast wave peak measured for AN/Al charges was lower than that for phlegmatized RDX (RDXph) charges of the same

[a] *W. A. Trzciński, K. Barcz, J. Paszula, S. Cudziło*
Military University of Technology
Advanced Technology and Chemistry
Kaliskiego 2
Warsaw 00908, Poland
**e-mail: wtrzcinski@wat.edu.pl*

 © 2014 Wiley-VCH Verlag GmbH & Co. KGaA, Weinheim

mass. However, the overpressure impulses were comparable and even larger for the AN/Al compositions.

The explosion of an annular charge composed of a RDXph core and a layer consisting of a mixture of ammonium nitrate (AN) and aluminum (Al) particles was studied in Refs. [7,8]. X-ray photography was used to trace the curvature of the shock wave in the external layer. The pressure blast characteristics and the light output of the explosion cloud were investigated using bunkers of different sizes and varying levels of the opening (the ratio of the hole surface to the total bunker surface). Overpressure peaks, the impulses of incident waves, and the impulses determined for the specified time duration were analyzed. It was found that the external layer composed of a mixture of fuel (Al) and oxidizer (AN) is compressed and dispersed by the shock wave and the expanding detonation products of the internal explosive charge. From an X-ray photo analysis, it appears that the detonation phenomenon does not occur in the external layer. The measured blast wave characteristics and the light outputs of explosion clouds confirm the ammonium nitrate decomposition and aluminum particle combustion during the explosion. The size of the used phlegmatized RDX core only slightly influences the aluminum combustion process after detonation of the layered charges in the bunkers. However, this influence can be observed in charges having the highest aluminum content (75 %) in the mixture with ammonium nitrate in the external layer. Finally, oxygen from air is used for aluminum particle combustion during the late stage of particle dispersion.

The present work is a continuation of the study presented in Refs. [7,8]. Ammonium perchlorate (AP) is used as an oxidant in the layered charge and an attempts is undertaken to assess the impact of the quantity and type of aluminum on the blast parameters. Influence of the experiment scale on the blast parameters is also examined. These studies were conducted in a semi-closed bunker. Measurements of a quasi-static pressure in a fully enclosed steel chamber were also performed. The morphology and composition of the solid products recovered from the chamber were determined.

2 Experimental Approach and Results

2.1 Characteristics of Layered Charges

Figure 1 shows a cross section of a cylindrical layered charge applied in tests. The charges used in research in the bunker had a core with a diameter $\Phi_1 = 25$ or 30 mm. The internal cylinder was composed of pellets of RDX phlegmatized by 6 wt.-% wax (RDXph). The pellets had a density of 1.67–1.68 g cm^{-3} and were glued together. RDXph cores weighed either 110 g or 190 g for smaller and larger diameter, respectively. The external charge included a combination of ammonium perchlorate (AP) and aluminum powder (Al). In this investigation, mixtures containing 25 and 50 wt. % of an oxidizer AP were used. Moreover, charges containing only Al powder were also tested. Crystalline ammonium perchlorate with particle sizes below 0.8 mm and two types of aluminum powder were used. The first one with particles below 44 μm (325 mesh) was designated hereafter as Al1 and the second with particle sizes between 44 and 149 μm (325 to 100 mesh) was marked as Al2. The mixtures were made using long-lasting mixing. A cylindrical charge was put into a paper tube having a thickness of 3 mm. The outer diameter Φ_2 was 40 mm for smaller charges and 50 mm for larger charges. Weight of the outer layer in the first case was 136 ± 2 g, while the other approximately 272 ± 3 g. The detonation of the inner core was initiated using a standard electrical detonator. For comparison with the smaller charges, the tests were carried out in the bunker for RDXph and TNT pressed charges of 247 g mass and 40 mm diameter. In layered charges used in the steel chamber the mass of RDXph core was 21 g and the core diameter was 16 mm. The mixture in the outer layer with a diameter of 30 mm had a weight of 40 g.

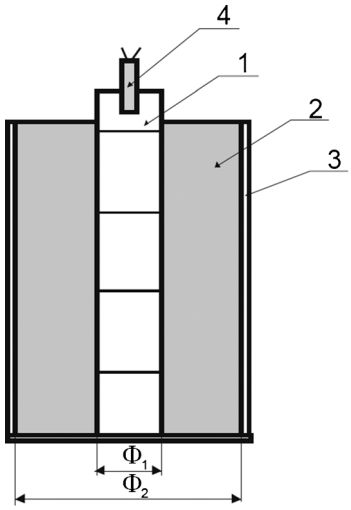

Figure 1. Schematic of the investigated layered charge: 1 – RDXph, 2 – mixture of AP/Al, 3 – paper tube, 4 – detonator, Φ_1 – diameter of the internal charge (25 or 30 mm), Φ_2 – internal diameter of the paper tube (40 or 50 mm).

2.2 Experimental Site

The experiments with larger charges were performed in the bunker which schematic and the locations of a charge and gauges are shown in Figure 2. The bunker has a volume of about 40 m^3, and it has four small openings each with a surface of 0.05 m^2 and a frontage opening with a surface about 1.3 m^2. Tested charge was placed 1.5 m above the ground in the bunker.

The blast pressure history was measured by piezoelectric gauges (137A21 or 137A22 from PCB Piezotronics, Inc.) fixed at distances 2 m and 2.5 m from the charge. Both gauges recorded the overpressure of an incident shock

 © 2014 Wiley-VCH Verlag GmbH & Co. KGaA, Weinheim

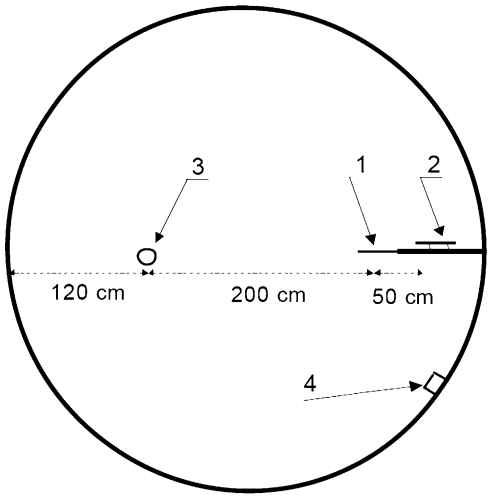

Figure 2. Schematic of the bunker with measurement equipment (top view): 1, 2 – pressure gauges, 3 – explosive charge, 4 – photodiodes.

wave, as it slid on the working surface of the devices. But later the waves reflected at the bunker wall and the ground loaded these devices at different angles. A photodiode BPDP35 was used to estimate the light output of the explosion charges. The output voltage of the used photodiode increases linearity with light intensity. The photodiode recorded the light passing through the air.

Quasi-static pressure (QSP) tests for the mixtures were performed in a chamber of about 0.15 m^3 volume. A schematic of the chamber is shown in Figure 3. The chamber was filled with air or argon under a normal pressure of about 0.1 MPa. The ambient temperature was about 20 °C. A charge was hung in the center of the chamber. A standard fuse was applied to initiate the detonator. A mass of 1.3 g of PETN can be assumed as an energetic equivalent of the explosive and firing composition of the detonator. Signals of overpressure from two piezoelectric gauges (M102A or M102A03 from PCB Piezotronics, Inc.) located at the chamber's wall were recorded by a digital storage scope. The gauges measured reflected overpressure. To reduce the vibrations from the chamber a Teflon sheet separating the chamber body from the transducer was applied. The transducers were also protected from heat transfer from the hot gases inside the chamber by a layer of black electrical tape.

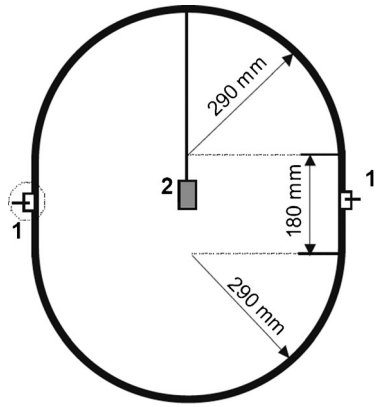

Figure 3. Schematic of the explosion chamber (side view): 1 – pressure gauges, 2 – explosive charge.

2.3 Exemplary Results

At least two tests were performed for each investigated explosive composition and charge. Exemplary blast wave measurements in the bunker are shown in Figure 4. Nearly the entire profile of the incident waves was undisturbed and recorded by both gauges. After some period of time (approx. 3 ms), the profile is perturbed by the shock waves reflected by the bunker wall. Unburned particles can also cause disturbances on the surface of pressure sensor. As shown in Refs. [9,10], agglomerates of solid particles from a layer dissipated by the products of explosion may even overtake the leading shock wave in the air. If the direction of their movement is not exactly perpendicular to the sensor surface, their impact can disrupt the overpressure measurement.

Typical light records measured during the explosions are presented in Figure 5. It can be assumed that the appearance of the signal corresponds to the initiation of explosion (negative value of time is due to the correlation of the beginning of time with the arrival of blast wave to the first sensor). The light output rapidly increases at the initial stage of explosion for all tested charges. The second increase is observed also at each light history. However, the signals for charges RDXph-Al/AP are much larger than those for RDXph and TNT charges.

Exemplary overpressure histories measured in the explosion chamber are shown in Figure 6. The main oscillations in the overpressure records are caused by shock wave re-

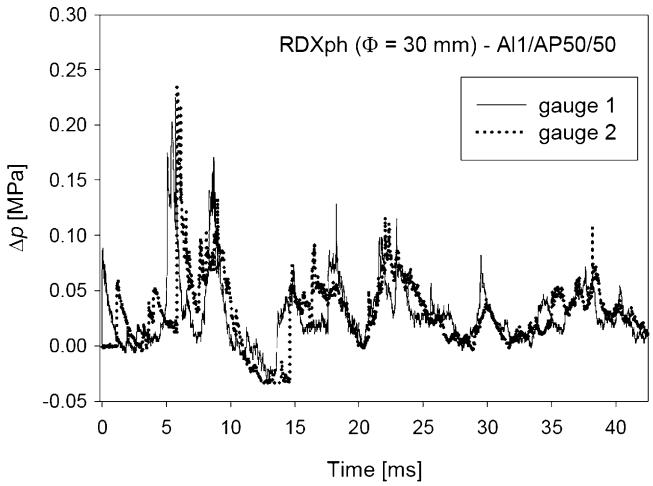

Figure 4. Overpressure measured in the bunker after the explosion of the layered charge: RDXph with a mixture AP/Al1 = 50/50.

 © 2014 Wiley-VCH Verlag GmbH & Co. KGaA, Weinheim

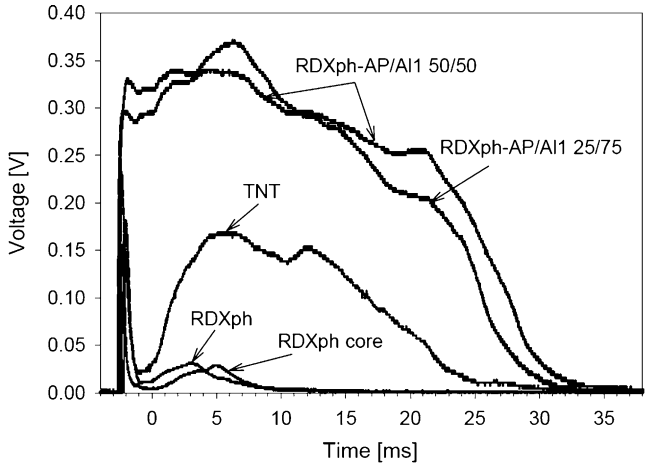

Figure 5. Light output records for chosen layered charges used in the bunker.

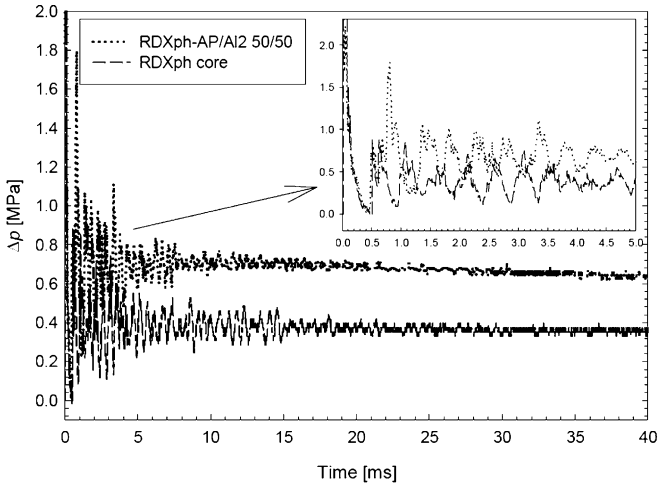

Figure 6. Exemplary overpressure histories recorded in the 0.15 m^3 chamber.

verberations at the chamber wall (see curves in the upper right corner in Figure 6). Their amplitudes decrease with time. There is also observed "noise" on pressure histories of smaller amplitude and higher frequency. These disturbances are the result of turbulence of gaseous medium, reverberations of shock waves inside the chamber sockets and vibration of the measuring system.

3 Blast Data Analysis

3.1 Tests in the Bunker

The time histories of pressure measured in the bunker after the detonation enable us to determine the characteristics of blast waves generated by layered charges. The maximum overpressure and specific impulse were determined directly from the experimental data.

The values of the overpressure peak and the specific impulse (obtained from the integration of the first peak of overpressure) for an incident blast wave are presented in Figure 7 and Figure 8 for the charges of $\Phi_2 = 40$ and in Figure 9 and Figure 10 for the charges of $\Phi_2 = 50$ mm. Additionally, Figure 7 and Figure 8 include values for the pressed charges of RDXph and TNT, with approximately the same mass of 247 g as in the smaller layered charges. For comparison, the results obtained for the RDXph cores are also presented in Figure 7, Figure 8, Figure 9 and Figure 10.

The analysis of Figure 7–10 shows that between charges of smaller and larger diameter the increase in parameters of the incident blast wave is visible by only 25–30% despite the fact that the weight of the RDXph core with outer layer for these charges differs twice. It was also observed that in practically all cases the blast wave parameters rise with increasing aluminum content, which is particularly evident in the case of charges with larger diameter core. This means

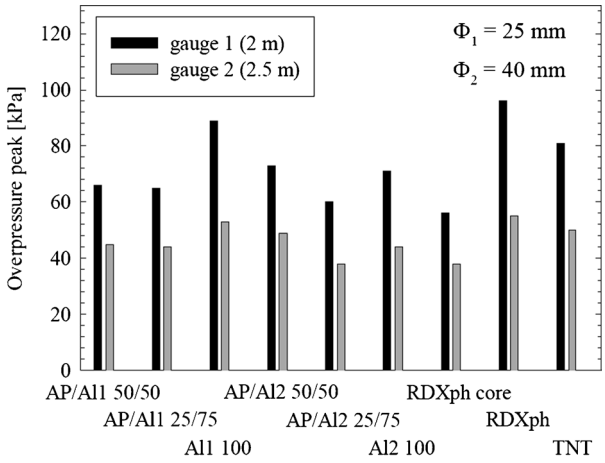

Figure 7. Peak overpressures of the incident blast waves for the charges of $\Phi_2 = 40$ mm.

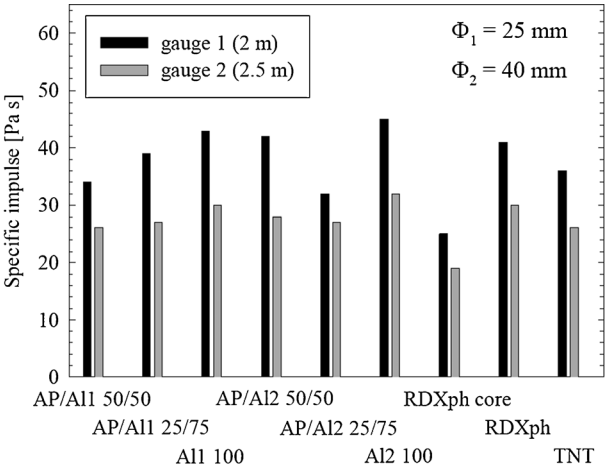

Figure 8. Specific impulses of the incident blast waves for the charges of $\Phi_2 = 40$ mm.

 © 2014 Wiley-VCH Verlag GmbH & Co. KGaA, Weinheim

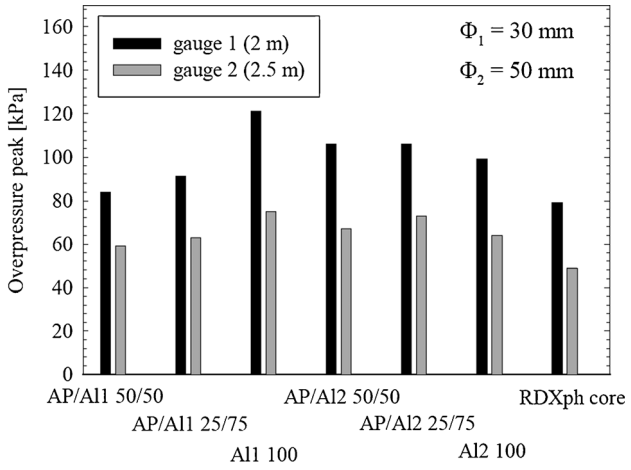

Figure 9. Peak overpressures of the incident blast waves for the charges of $\Phi_2 = 50$ mm.

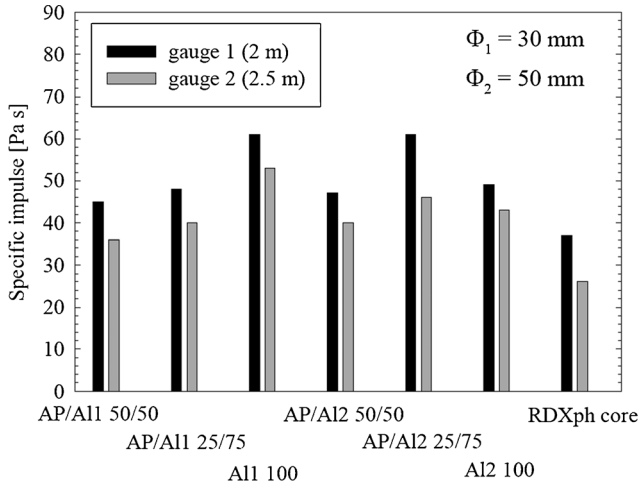

Figure 10. Specific impulses of the incident blast waves for the charges of $\Phi_2 = 50$ mm.

that aluminum reacts with the products of detonation of RDXph, AP decomposition products and oxygen from the air. The latter reaction is apparent in high parameters of blast waves recorded for the charges RDXph-Al (without AP).

From the data given in Figure 7–10 follows that the question which of the powder ensures better blast performance (overpressure peak and specific impulse) of the tested charges is without a clear answer. The reason may be that the measurements of rapid changes of pressure in the blast wave using piezoelectric sensors are performed with some error and that only two tests were performed for each explosive.

The blast overpressure in semi-closed structures can be characterized by the impulse defined in Equation (1).

$$I = \int_0^t \Delta p(\tau) d\tau \quad (1)$$

where $\Delta p(\tau)$ is the overpressure history and t denotes time. The histories of the impulses calculated for a time period of about 40 ms after the shock wave reached the gauges in the bunker were compared. This time period was chosen because the results at later time are not repeatable. A thorough analysis of the results obtained does not clearly determine the effect of the type of aluminum powder on the total pressure impulse. So, the exemplary impulse histories are compared in Figure 11, Figure 12, Figure 13, and Figure 14 only for the charges with Al1. There is a clear growing trend in impulses measured by both sensors with increasing aluminum content in an outer layer. For charges with almost twice as much weight a clear increase in pulse pressure specified for the time $t = 40$ ms can be seen. For most explosive systems investigated, it is from 80 to 100 %. The highest values of the impulse were obtained for layered charges containing only aluminum powder.

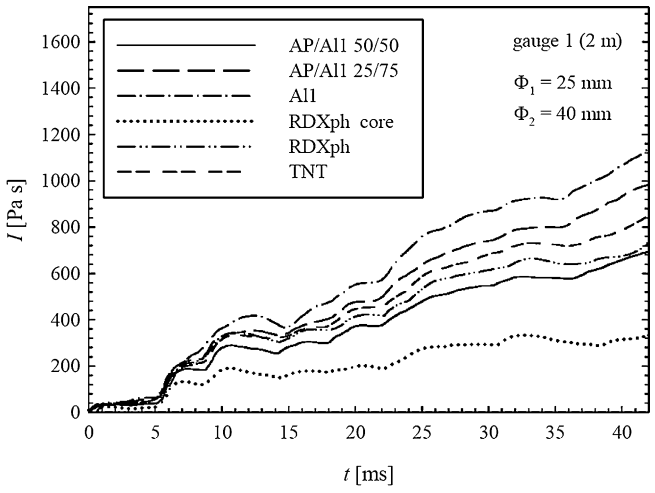

Figure 11. Impulse histories at a distance 2 m for the 40 mm diameter charges with Al1 powder.

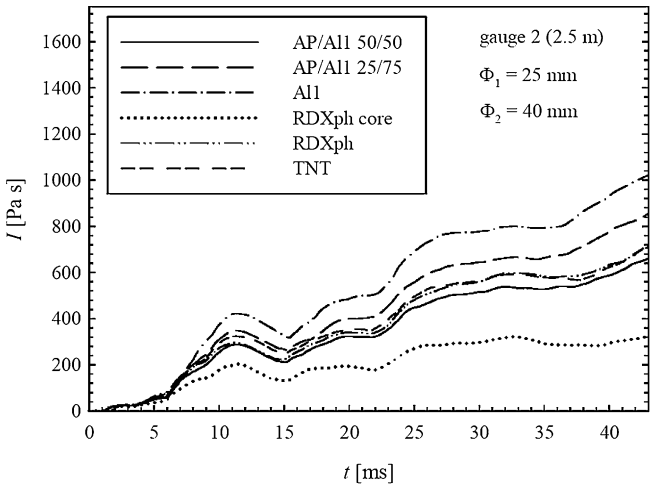

Figure 12. Impulse histories at a distance 2.5 m for the 40 mm diameter charges with Al1 powder.

 © 2014 Wiley-VCH Verlag GmbH & Co. KGaA, Weinheim

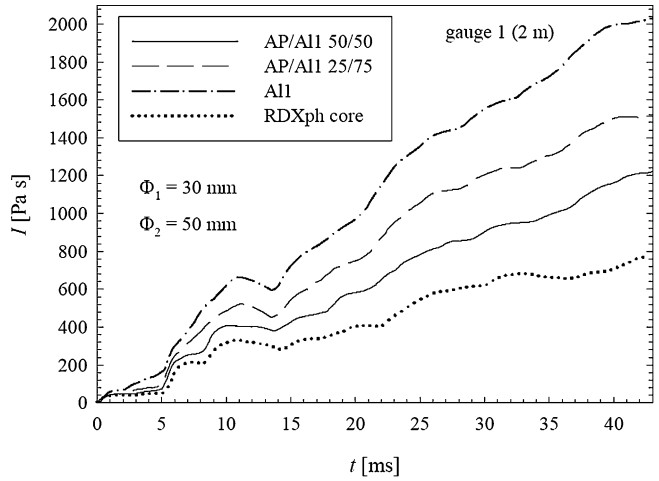

Figure 13. Impulse histories at a distance 2 m for the 50 mm diameter charges with Al1 powder.

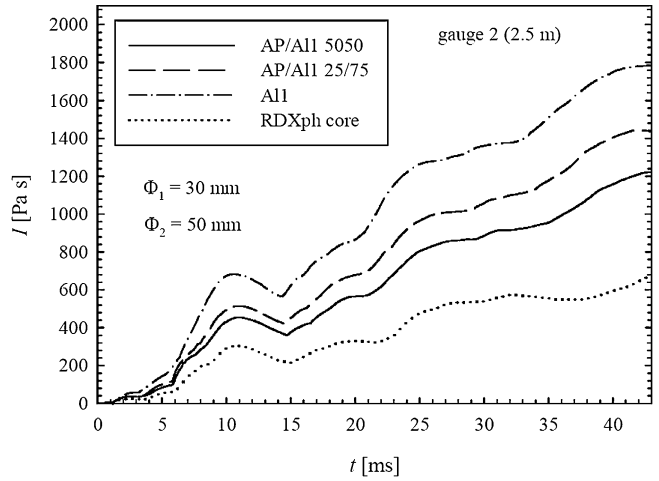

Figure 14. Impulse histories at a distance 2.5 m for the 50 mm diameter charges with Al1 powder.

There are slightly larger values of the total impulse calculated for sensor located closer to a charge (2 m). It is somewhat startling conclusion, because blast waves propagate at approximately the same distances, and the pressure levels out with time in the bunker. Probably the values of the specific impulses influence this difference.

Table 1 summarized the average values of light output of the cloud of detonation products recorded during an explosion in the bunker. Burn time of explosion of tested layered charges is similar. However, in comparison with the charges containing pure RDXph for all other charges this time has been extended 3–4 times, which confirms that the aluminum powder burns during the explosion. In the case of TNT, the light output increases as a result of the combustion of unburned carbon in air.

Table 1. The light output of the explosion cloud of reactive products obtained from the photodiode.

Charge	Light output [ms]	
	$\Phi_1 = 25$ mm	$\Phi_1 = 30$ mm
RDXph core	8	11
RDXph	7	–
TNT	26	–
AP/Al1 50/50	32	31
AP/Al1 25/75	30	29
Al1 100	–	26
AP/Al2 50/50	26	27
AP/Al2 25/75	27	26
AL2 100	23	27

3.2 Tests in the Chamber

Pressure histories measured in the explosion chamber were approximated by using the function Equation (2).

$$\Delta p_{apr} = a\left(1 - e^{-bt}\right) + c\,e^{-dt} \tag{2}$$

where *a*, *b*, *c* and *d* are constants. The first part describes the growth of the average pressure in the chamber due to combustion of aluminum particles in the air and detonation products, the second one is responsible for the drop in pressure caused by the transmission of heat from the gaseous medium to the steel wall of the chamber. Function (2) reaches a maximum value Δp_{max} for time t_{max} Equation (3).

$$t_{max} = \ln\left(\frac{a\,b}{c\,d}\right)\frac{1}{b-d} \tag{3}$$

Values of Δp_{max} determined on the basis of at least six pressure histories measured in the chamber filled with air are summarized in Table 2. The values of overpressure estimated in this way can be treated as a quasistatic pressure (QSP). The Table also provides values of overpressure Δp_{cal} calculated for the constant-volume explosion of the charges in the chamber with air (no heat loss to the wall of the

Table 2. Values of Δp_{max} obtained from the over-pressure histories measured in the chamber with air and calculated by using CHEETAH code.

Charge	Δp_{max}	Δp_{cal}	$\Delta p_{max}/\Delta p_{cal}$
	[MPa]	[MPa]	[%]
RDXph core	0.42 ± 0.02	0.54	77.8
AP/Al1 50/50	0.78 ± 0.07	1.17	66.7
AP/Al2 50/50	0.78 ± 0.05		66.7
AP/Al1 25/75	0.81 ± 0.07	1.27	63.8
AP/Al2 25/75	0.79 ± 0.04		62.2
Al1 100	0.75 ± 0.07	1.33	56.4
Al2 100	0.73 ± 0.05		54.9

© 2014 Wiley-VCH Verlag GmbH & Co. KGaA, Weinheim

chamber). Calculations were performed using the CHEETAH code [11].

The data presented in Table 2 show that the use of the outer layer increases twice the quasistatic pressure. However, the measured values of this pressure are much lower than the calculated average pressures in the chamber. The ratio of the measured and calculated pressures decreases with increasing content of aluminum powder in the layered charge. Since the thermochemical calculations show that the total amount of aluminum burns up during the explosion in the chamber, this means that in real conditions only a portion of aluminum reacts with oxygen from the RDX detonation products, AP and air during the measurement of overpressure (40 ms). Noteworthy is the fact that, for charges containing aluminum without additional oxidizer (AP) the obtained value of QSP are only slightly lower than that for the charges with an AP-Al layer.

Measurements results for the chamber filled with argon are shown in Table 3. The results of calculations are also presented. The equilibrium pressure was calculated with assumption of the chemical activity or chemical inertness of aluminum, $\Delta p_{cal/a}$ and $\Delta p_{cal/in}$, respectively. Lack of oxygen from air causes that the measured QSP decreases with increasing Al contents in mixtures with AP. Pressure measured for the charge containing pure aluminum is slightly lower than that specified for the RDX core and is close to the pressure calculated by assuming an inertial aluminum.

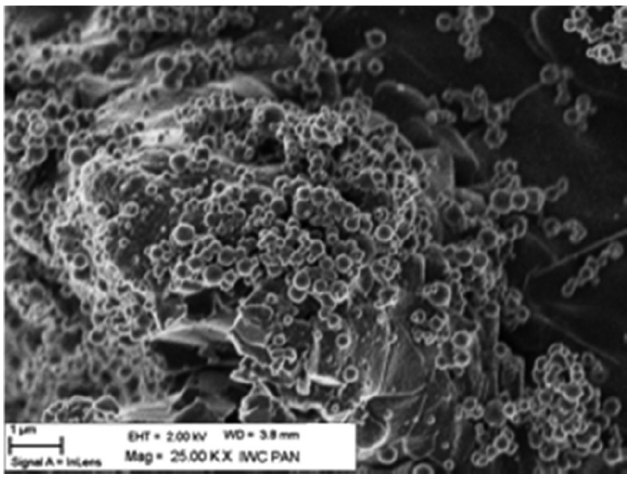

Figure 15. SEM image of the solid product of the charge with AP/Al1 25/75 mixture.

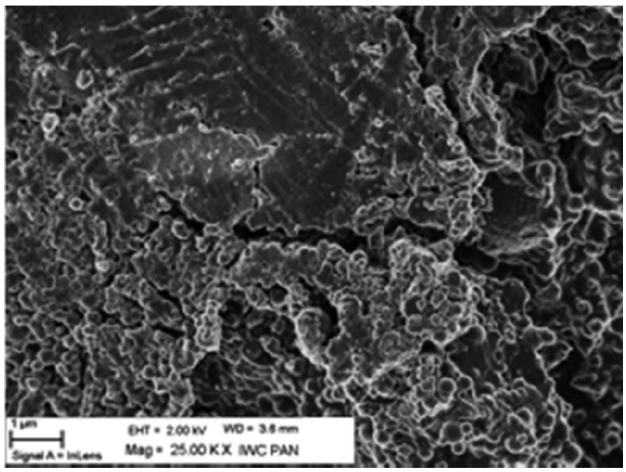

Figure 16. SEM image of the solid product of the charge with AP/Al2 25/75 mixture.

4 Analysis of Solid Products of Explosion

Solid explosion products recovered from the chamber after explosions of the tested charges in air or argon atmosphere were washed with water, dried at 100 °C for 4 h, and analyzed in order to determine their morphology as well as chemical and phase compositions.

4.1 SEM Analysis

High resolution scanning electron microscopy (LEO 500 operating at 20 kV) was used to study the morphology of solid explosion products. Exemplary HR SEM images of the solid residues from the chamber filled with air are shown in Figure 15, Figure 16, Figure 17, and Figure 18.

Spherical particles with diameters lower than 1 µm are visible in all the samples recovered from the chamber with air. They are located on the surface of larger particles. These regular submicron spheres are most probably alumi-

Table 3. Values of Δp_{max} obtained from the over-pressure histories measured in the chamber with argon and calculated $\Delta p_{cal/a}$, $\Delta p_{cal/in}$.

Charge	Δp_{max} [MPa]	$\Delta p_{cal/a}$ [MPa]	$\Delta p_{max}/\Delta p_{cal/a}$ [%]	$\Delta p_{cal/in}$ [MPa]	$\Delta p_{max}/\Delta p_{cal/in}$ [%]
RDXph core	0.36 ± 0.01	0.40	90.0	0.40	90.0
AP/Al1 50/50	0.79 ± 0.05	1.21	65.3	0.69	114.5
AP/Al2 50/50	0.76 ± 0.01		62.8		110.1
AP/Al1 25/75	0.58 ± 0.01	0.95	61.1	0.47	123.4
AP/Al2 25/75	0.57 ± 0.01		60.0		121.3
Al1 100	0.26 ± 0.01	0.79	32.9	0.28	92.9
Al2 100	0.30 ± 0.04		38.0		107.1

 © 2014 Wiley-VCH Verlag GmbH & Co. KGaA, Weinheim

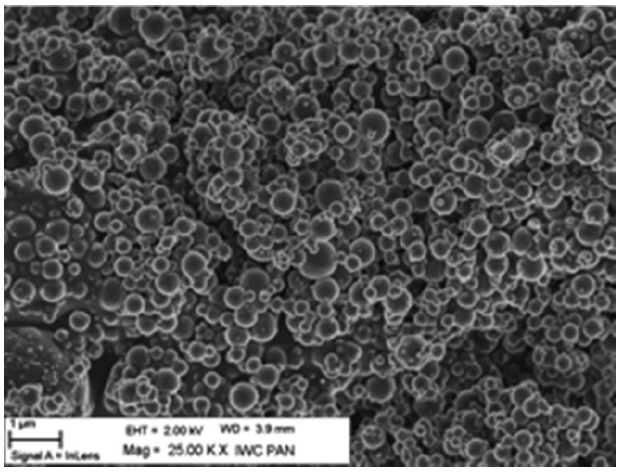

Figure 17. SEM image of the solid product of the charge with Al1 powder.

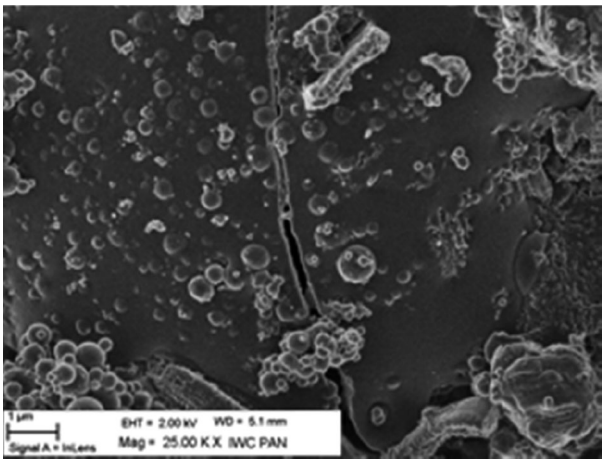

Figure 18. SEM image of the solid product of the charge with Al2 powder.

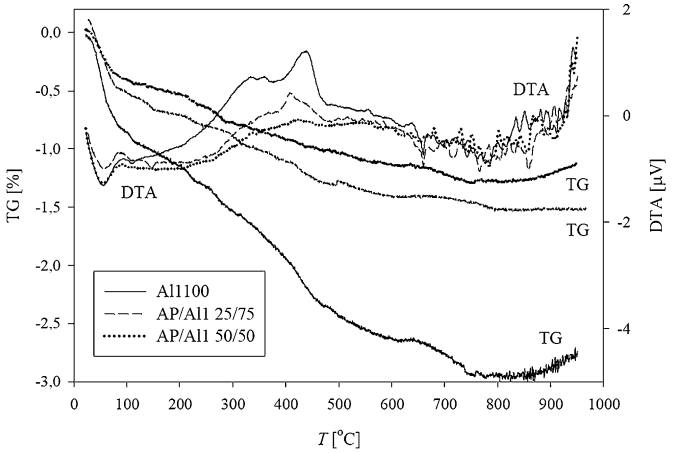

Figure 19. TG/DTA curves for residues of charges containing Al1 (air in the chamber).

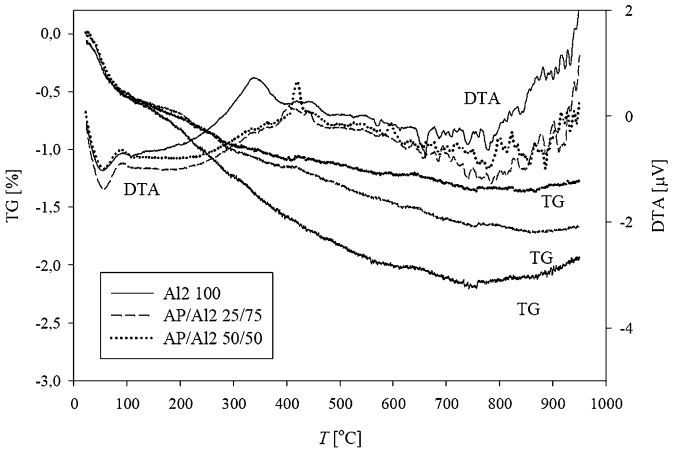

Figure 20. TG/DTA curves for residues of charges containing Al2 (air in the chamber).

num oxide particles formed by oxidation of melted aluminum droplets with gaseous oxygen in a process of the so-called filtration combustion. This means that the heat of explosion in air was sufficient to increase the temperature of a part of the aluminum particles above the melting point of aluminum. In the case of solid products of explosions in argon the particles are smaller, agglomerated and not so regular in shape. They may be just partly oxidized aluminum particles.

4.2 DTA/TG Measurements

Simultaneous TG/DTA measurements were performed using a Labsys TG/DTA-DSC apparatus (SETARAM). Runs were carried out using opened alumina crucibles with Al_2O_3 in the reference pan. Powdery samples of the detonation products were from 28 to 39 mg in mass. All the TG/DTA traces were recorded at 10 K min^{-1} heating rate in a synthetic air dynamic atmosphere (N_2/O_2 79/21 in volume, flow rate 50 mL min^{-1}.). The obtained thermograms for samples extracted from the chamber filled with air are presented in Figure 19 and Figure 20.

Analysis of the TG curves indicates that during heating in air the samples systematically lose their weight. In a temperature range of 20–120 °C, the sample mass diminishes by 0.5–1 %. This is an endothermic process (minima are visible on the DTA curves), so that it is caused by evaporation of adsorbed gases and water. Above 200 °C, carbonaceous products of the explosives decomposition begin to oxidize, what is evidenced by the slow decrease in mass of the samples and the presence of a broad, exothermic peak on the DTA curves.

The highest mass reduction (2–3 %) was measured for the explosion products of charges containing exclusively aluminum powder (Al1 or Al2) in the outer layer. Addition of ammonium perchlorate to aluminum powder reduces the contents of unburned substances in the explosion products owing to an increase in the oxygen concentration

 © 2014 Wiley-VCH Verlag GmbH & Co. KGaA, Weinheim

in the post-explosion cloud. As it should be expected, the more AP in the external layer is (25 or 50%), the lower weight loss is.

Metallic aluminum also remains inside aluminum oxide particles formed in the explosion of charges without AP. This is evidenced by a small Al melting endotherm peaking at approx. 660 °C. Melted aluminum is not oxidized instantly because is covered with a thick layer of aluminum oxide that prevents its oxidation (no mass increase up to approx. 850 °C).

When the tested charges were detonated in an argon atmosphere, more unburned aluminum and carbonaceous materials were detected in the solid explosion products. From the thermograms presented in Figure 21 and Figure 22, it follows that the mass of the samples decreases by 4 to 8% when heated in air up to 500 °C. Obviously, it is particularly evident for the explosion products of charges without the oxidizer.

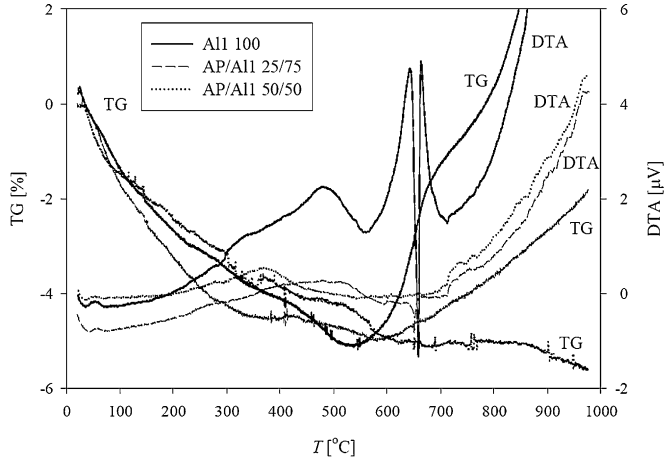

Figure 21. TG/DTA curves for residues of charges containing Al1 (argon in the chamber).

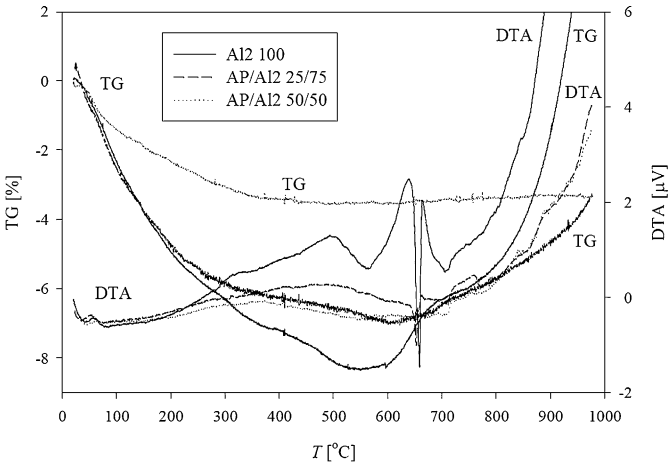

Figure 22. TG/DTA curves for residues of charges containing Al2 (argon in the chamber).

During heating in air, aluminum starts to oxidize at approx. 550 °C (the onset of a large exothermic peak on the DTA curve), and next melts after reaching a temperature of approx. 655 °C (sharp endotherm peaking at 660 °C). Of course Al oxidation results in a significant increase of the sample mass (by approx. 7% at 800 °C), as evidenced by the TG traces. Contrary to the products of explosion in air, the oxidation process of Al particles remaining after explosion in argon begins at a temperature of 550 °C, i.e. lower than melting point of aluminum, so that the particles were not covered with thick alumina layers.

Also in this case the presence of AP in the charges causes that more aluminum reacts in the explosions, and when the contents of AP is 50%, aluminum is completely oxidized. On the corresponding DTA traces, there is neither Al oxidation exotherm nor Al melting endotherm, and the mass of the samples does not practically change in a temperature range of 600 to 1000 °C.

4.3 XRD Analysis

The composition of the solid products was studied by means of X-ray diffraction (XRD) technique (Siemens Diffractometer D500 with Cu K_α radiation). For the analysis of the spectra obtained ICDD database PDF4+ (2009) of standard diffraction patterns was used.

The phases identified in the solid residue from the chamber filled with air are presented in Table 4. The Table shows that the different forms of alumina are present in the explosion products, and in one case, the iron oxide (the chamber is made of steel). Alumina have different crystal structure: rhombohedra (corundum – 46-1212), cubic (10-425, 50-741) and orthorhombic (46-1215). The estimated crystallite size of corundum is in the range 40 to 50 nm. The crystallites for other phases are smaller, but their size is difficult to estimate. In all samples, there are no crystallites of metallic Al.

The thermochemical calculations performed by using the CHEETAH code shows that the temperature of an ideal explosion in the chamber with air is 1639, 3104, 3539 and 3915 K, respectively for a charge of pure RDXph and for charges consisting of mixtures of AP/Al = 50/50, AP/Al = 25/75 and aluminum powder in the outer layer. However, it must be noted that the parameters are calculated for the explosion for ideal mixing of the reactants. Assuming that only part of the aluminum will burn in the initial phase of mixing of the explosion products and air, it can be assumed that, in the case of layered charge, the average temperature of the reactive mixture is higher than 930 K, i.e. above the melting point of aluminum. Thus, aluminum powder should burn in oxygen from the air enclosed in the chamber. This is confirmed by the results of the TG/DTA and XRD analyses presented above.

The results of XRD analysis for the samples from the chamber filled with argon are presented in Table 5.

 © 2014 Wiley-VCH Verlag GmbH & Co. KGaA, Weinheim

Table 4. Phases matched in the solid products retrieved from the chamber filled with air.

External charge	Matched phases		
	Aluminum oxide	Aluminum	Iron oxide
AP/Al1 50/50	46–1212 50–0741	No	no
AP/Al2 50/50	46–1212 50–0741	No	no
Al1 100	10–0425 46–1212	No	280491
Al2 100	46–1212 50–0741 46–1215	No	no

Table 5. Phases matched in the solid products retrieved from the chamber filled with argon.

External charge	Matched phases				
	Aluminum oxide	Aluminum	Iron	Aluminum oxide nitride	Aluminum oxide carbide
AP/Al1 50/50	46–1212 46–1215	no	No	18–0052	no
AP/Al2 50/50	46–1212 46–1215 50–1215	no	No	no	no
AP/Al1 25/75	46–1212	04–0787	06–0696	18–0052	36–0148
AP/Al2 25/75	46–1212	04–0787	No	18–0052	36–0148
Al1 100	no	04–0787	06–0696	18–0052	no
Al2 100	50–0741 05–0712	04–0787	06–0696	no	no

Metallic aluminum is present in the residue after detonation of charges containing the mixture AP/Al with 75% aluminum and pure aluminum. Moreover, the residue contains aluminum oxide nitride and aluminum oxide carbide. In the case of a mixture including 50% AP, aluminum is not present in the product. The main phases matched in the products are different forms of alumina, like in the chamber filled with air.

5 Conclusions

Analysis of the results obtained in the work leads to the following conclusions:

1. The parameters of the incident blast wave increased by only 25–30% after the explosion of larger layered charges inside the bunker despite the fact that the charge weight increased twice.
2. The blast wave parameters increase with the increase of aluminum contents, particularly in the case of charges with larger diameter core. This means that aluminum burns, and additional heat strengthens the blast wave already during the detonation products expansion.
3. Due to the dynamic changes in overpressure the question is not answered how the particle size of aluminum affect the blast wave parameters of the tested charges.
4. The increase in the total pressure impulse in the bunker, determined for the time of about 40 ms, for almost all large charges is about 80–100% in relation to small charges weighing two times less. The highest impulses were obtained for charges with the outer layer of pure-aluminum powder.
5. Light output time of explosion of the layered charges was 3–4 times longer than the RDXph core.
6. As compared to the core, the application of the outer layer in the charges causes twofold increase in quasi-static pressure inside the chamber filled with air.
7. The values of a ratio of the quasistatic pressure to the average pressure obtained from thermochemical calculation show that only part of the aluminum burns up during the measurement time of overpressure in the chamber (40 ms).
8. Lack of oxygen from air causes that the QSP in the chamber filled with argon decreases with increasing Al contents in mixtures with AP.
9. From the TG/DTA and XRD analysis of the chamber residue it follows that the aluminum powder is almost completely burned after the explosion of the layered charges in air.

© 2014 Wiley-VCH Verlag GmbH & Co. KGaA, Weinheim

10. Metallic aluminum is present in the residue after detonation of charges with Al and AP/Al 25/75 in the chamber filled with argon.

Acknowledgments

This paper was based on works presented at the 14th Seminar on New Trends in Research of Energetic Materials, Pardubice, Czech Republic, 13–15 April, 2011, and at the 22nd International Symposium on Military Aspects of Blast and Shock, Bourges, France, 4–9 November, 2012.

References

[1] M. L. Chan, G. W. Meyers, *Advanced Thermobaric Explosive Compositions*, US Patent 6,955,732 B1, Ridgecrest, CA, USA, **2005**.
[2] M. L. Chan, D. T. Bui, G. Meyers, A. Turner, *CasTable Thermobaric Explosive Formulations*, US Patent 6,969,434 B1, Ridgecrest, CA, USA, **2005**.
[3] R. H. Guirguis, *Reactively Induced Fragmenting Explosives*, US Patent 6,846,372 B1, FairFax, VA, USA, **2005**.
[4] A. Hahma, K. Palovuori, Y. Solomon, TNT-Equivalency of Thermobaric Explosives, *36th Int. Annual Conference of ICT*, Karlsruhe, June 28–July 1, **2005**, V10-1.
[5] J. M. Peuker, H. Krier, N. Glumac, Particle Size and Gas Environment Effects on Blast and Overpressure Enhancement in Aluminized Explosives, *Proc. Combust. Inst.* **2013**, *34*, 2005.
[6] J. Paszula, W. A. Trzciński, K. Sprzątczak, Detonation Performance of Aluminum-Ammonium Nitrate Explosives, *Cent. Eur. J. Energ. Mater.* **2008**, *5*, 3.
[7] W. A. Trzciński, K. Barcz, Investigation of Blast Wave Characteristics for Layered Thermobaric Charges, *21st International Symposium on Military Aspects of Blast and Shock*, Jerusalem, Israel, 3–8 October **2010**, p. 97–1(CD).
[8] W. A. Trzciński, K. Barcz, Investigation of Blast Wave Characteristics for Layered Thermobaric Charges, *Shock Waves*, **2012**, *22*, 119.
[9] S. Goroshin, D. L. Frost, R. Ripley, F. Zhang, Measurement of Particle Density During Explosive Particle Dispersal, *21st International Symposium on Military Aspects of Blast and Shock*, Jerusalem, Israel, 3–8 October,**2010**, p. 98–1(CD).
[10] M. O. Sturtzer, Y. Gregoire, D. Eckenfels, Experimental Study of Aluminum Particles Dispersed and Ignited by High Explosives, *21st International Symposium on Military Aspects of Blast and Shock*, Jerusalem, Israel, 3–8 October,**2010**, p. 33–1(CD).
[11] L. E. Fried., *CHEETAH 1.39 – User's Manual, Manuscript UCRL-MA-117541 Rev.3*, Lawrence Livermore National Laboratory, CA, USA, **1996**.

Received: January 25, 2013
Revised: July 17, 2013
Published online: October 9, 2013

 © 2014 Wiley-VCH Verlag GmbH & Co. KGaA, Weinheim